Phytochemistry 178 (2020) 112459

Contents lists available at ScienceDirect

Phytochemistry

journal homepage: www.elsevier.com/locate/phytochem

Diterpenoid alkaloids from *Aconitum anthoroideum* that offer protection against MPP^+–Induced apoptosis of SH–SY5Y cells and acetylcholinesterase inhibitory activity

Shuai Huang, Ji-Fa Zhang, Lin Chen, Feng Gao, Xian-Li Zhou *

School of Life Science and Engineering, Southwest Jiaotong University, Chengdu, 610031, Sichuan, PR China

ARTICLE INFO

Keywords:
Aconitum anthoroideum DC.
Ranunculaceae
Diterpenoid alkaloids
Anthoroidine a
Anthoroidine B
Neuroprotective activities
Acetylcholinesterase inhibitory effects

ABSTRACT

Nine unprecedented diterpenoid alkaloid, including a diterpenoid alkaloid featuring a diterpenoid moiety, anthoroidine A; one bisditerpenoid alkaloid joined with a carbon–carbon single bond, anthoroidine B; three racemulosine-type C_{20}-diterpenoid alkaloids, anthoroidines C–E; one hetidine-type C_{20}-diterpenoid alkaloid, anthoroidine F; and three hetisine-type C_{20}-diterpenoid alkaloids, anthoroidines G-I, together with ten known diterpenoid alkaloids were isolated from *Aconitum anthoroideum* DC. Their structures were established via detailed spectroscopic analyses. Most of the isolated compounds along with five known diterpenoid alkaloids obtained in a previous study were screened for neuroprotective activities and acetylcholinesterase inhibitory effects. Nominine showed potent protective activity against MPP^+–induced apoptosis in SH–SY5Y cells, with a rescue rate of 34.4% (50 μM). Rotundifosine F showed a significant inhibitory activity against AChE (IC_{50} = 0.3 μM). The structure–activity relationship of these alkaloids is also briefly discussed.

1. Introduction

Alzheimer's disease (AD) and Parkinson's disease (PD), the most common progressive neurodegenerative diseases (NDs) impairing memory, cognition and movement, are an important modern health problem because they affect millions of people (primarily in the aging population) worldwide, and the number of patients is growing every day (Tarasoff-Conway et al., 2015; Shihabuddin et al., 2018). These conditions have an enormous global impact estimated to be more than $604 billion, affecting not only patients but also caregivers, who are usually family members (Alzheimer's Association, 2018; Betarbet et al., 2000). There is an urgent need to discover efficient therapeutic drugs that can block or delay the progressive loss of neurons.

Natural herbal products play a vital role in drug discovery (Ibrahim et al., 2013; Malak et al., 2018). Diterpenoid alkaloids, the main characteristic constituents of the genera *Aconitum* and *Delphinium*, possess interesting bioactivities, such as antiepileptiform, antioxidant, anti–inflammatory, analgesic, antiarrhythmia, antifungal, and cytotoxic properties, as well as being an antagonist of the neuronal nicotinic acetylcholine receptor (Wang et al., 2010; McKay et al., 2007). However, only a small proportion of alkaloids have been investigated for their neuroprotective activities and cholinesterase inhibitory effects (Ahmad et al., 2017a, 2017b,Atta–ur–Rahman et al., 2000).

Aconitum anthoroideum DC., belonging to the family Ranunculaceae, is mainly distributed in the Xinjiang Uygur region (Wang, 1979), and its bioactive constituents have not yet been reported. As part of our ongoing research program toward discovering structurally intriguing and biologically important diterpenoid alkaloids from the *Aconitum* and *Delphinium* genera, we studied the whole plants of *A. anthoroideum*, which led to the isolation of nine unprecedented diterpenoid alkaloids, namely anthoroidines A–I (**1**–**9**), together with ten known compounds, tanguticuline E (**10**) (Fan et al., 2019), hetidine hydrochloride (**11**) (Pelletier et al., 1970), hetisinone (**12**) (Gonzalez et al., 1986), hetisine (**13**) (Jiang and Pelletier, 1991), tadzhaconine (**14**) (Yusupova et al., 1992), (+)–(13*R*,19*S*)–1β,11α–diacetoxy–2α–benzoyloxy–13,19–dihydroxyhetisan (**15**) (Jiang et al., 2012), trifoliolasine E (**16**) (Zhou et al., 2005), atisinium chloride (**17**) (Pelletier and Mody, 1979), nominine (**18**) (He et al., 1997), and aconicarmicharcutinium A hydrochloride (**19**) (Meng et al., 2017a, 2017b). The protective effects against MPP^+–induced apoptosis in SH–SY5Y cells and the acetylcholinesterase (AChE) inhibitory activities of these isolated compounds along with five known diterpenoid alkaloids, rotundifosine E (**20**),

* Corresponding author. Natural Products Laboratory of School of Life Science and Engineering, Southwest Jiaotong University, Chengdu, 610031, Sichuan, PR China.
E-mail address: zhouxl@swjtu.edu.cn (X.-L. Zhou).

https://doi.org/10.1016/j.phytochem.2020.112459
Received 2 March 2020; Received in revised form 8 July 2020; Accepted 12 July 2020
Available online 23 July 2020

rotundifosine F (**21**), rotundifosine G (**22**), atidine (**23**), and ajaconine (**24**), obtained in our previous phytochemical studies of *Aconitum rotundifolium* (Zhang et al., 2019), were evaluated. Herein, the isolation and structural elucidation of these alkaloids as well as the biological evaluation of these compounds are described.

2. Results and discussion

2.1. Structure elucidation and identification

Compound **1**, an amorphous solid, displayed a protonated molecular ion at *m/z* 626.3845 $[M + H]^+$ in its HRESIMS spectrum (calcd. 626.3845), corresponding to the molecular formula $C_{40}H_{51}NO_5$. Its IR spectrum showed absorption bands for hydroxy (3393 cm^{-1}), carbonyl (1723 cm^{-1}) and carbon–carbon double bond (1666 cm^{-1}) functional groups. The NMR data (Table 1) of **1** exhibited signals characteristic of a trisubstituted double bond [δ_H 5.63 (s); δ_C 128.0 (d), 146.3 (s)], an exocyclic double bond [δ_H 4.70 (s), 4.89 (s); δ_C 109.1 (t), 143.6 (s)], two tertiary methyl groups [δ_H 0.98 (s) and 1.15 (s); δ_C 24.2 (q), 29.5 (q)], one aldehyde moiety [δ_H 9.85 (s); δ_C 206.7 (d)], a ketone group [δ_C 227.3 (s)], and an oxygenated methylene carbon [δ_H 3.87 (d, J = 14.2 Hz), and 4.17 (d, J = 14.2 Hz); δ_C 68.8 (t)]. Further analysis of the ^{13}C NMR, DEPT and HSQC data of **1** revealed that the unassigned carbon signals could be attributed to eleven methylenes, fourteen sp^3 methines (three oxygenated) and six sp^3 quaternary carbons. These features suggested that **1** consists of a C_{20}–diterpenoid alkaloid moiety (in black) and a diterpenoid (in blue) fragment (Wang and Liang, 2002).

The diterpenoid alkaloid moiety was deduced as hetisine (Jiang and Pelletier, 1991) by the similarities in their 1D and 2D NMR data. The ketone group (δ_C 227.3) in the diterpenoid moiety was assigned to C–20′ by the H–1′/C–20′ and H–13′/C–20′ HMBC correlations. The correlations observed in the HMBC experiment between the signals at δ_H 1.20 (H–3′), 1.54 (1H, m, H–5′), and 0.98 (3H, s, H–18′) with δ_C 206.8 allowed the assignment of the aldehyde group at C–19′. Comparing the spectroscopic data of the diterpenoid moiety in **1** with those of campylopin (Wang and Yan, 2007), a hetidane–type diterpene isolated from *Delphinium campylocentrum*, indicated that they have the same molecular skeleton. The main difference was that the acetyl and hydroxyl groups at C–7′ and C–15′ in campylopin were both substituted by hydrogen atoms in **1**. In addition, the expected exocyclic double bond was isomerized to the C–15′–C–16′ endocyclic double bond, and this is strongly supported by the HMBC cross–peaks of H–15′/C–7′, H–15′/C–17′, and H–17′/C–12′. Additionally, the HMBC correlations of H–17′ with C–2, C–15′ and C–12′, and of H–2 with C–10 and C–4 implied that the non–alkaloid part was linked with the alkaloid part via a C–17′–O–C–2 ether linkage. Accordingly, the complete planar structure of **1** was further verified by analysis of the HMBC, HMQC, and ^1H–^1H COSY spectra (Fig. S1).

The relative configuration of **1** was established through analysis of the coupling constants and key NOESY correlations (Fig. S2). The 18′–methyl group was assigned as β–oriented due to the correlations of H–18′ with H–6′β, H–3′β and H–5′β in the NOESY spectrum. As a consequence, H–19′ was assigned as being α–oriented, which was also supported by the correlations between H–19′ and H–2′α. The correlations of H–3′β/H–1′β, H–9′/H–1′β, H–7′β/H–9′, and H–5′/H–7′β indicated that H–5′ and H–9′ were also β–oriented. Comparison of the chemical shift and peak shape of H–2 (δ_H 4.16, br. S) with those of known hetisine–type alkaloids (Bessonova and Saidkhodzhaeva, 2000) suggested that the hydrogen at C–2 should be β–oriented. The large coupling constant of H–13 (J = 8.4 Hz) with H–14α revealed that the dihedral angle between these two H–atoms was *ca.* 0 °C, which implied that H–13 was in an α–orientation. The NOESY correlation of H–11 with H–15β indicated the β–orientation of H–11. Since the absolute configuration of hetisine was confirmed by X–ray crystallographic analysis (Tashkhodzhaev et al., 1992), it was proposed that the diterpenoid alkaloid substructure in **1** had the same absolute configuration. Hence, the structure of compound **1** was determined as shown in Fig. 1, and it was named anthoroidine A.

A plausible biogenetic pathway for **1** was proposed and is shown in Fig. 2. A hetidane–type diterpene (I) could be oxidized to corresponding epoxide II. Subsequently, a nucleophilic primary hydroxyl group of hetisine could attack the oxirane moiety of II, generating corresponding conjugated diterpenoid alkaloid III, which could be converted to anthoroidine A by the elimination of water.

Table 1
NMR Data for Compounds **1** and **2** (^1H: 600 MHz, ^{13}C: 150 MHz; δ in ppm, J in Hz).

No.	1 (in $CDCl_3$)		2 (in CD_3OD)	
	δ_H	δ_C, type	δ_H	δ_C, type
1	α 1.67 m β 3.17 d (15.6)	28.9, CH_2	α 1.73 m β 1.51 m	29.2, CH_2
2	3.71 br. s	72.8, CH	α 1.20 m β 1.53 [a]	21.9, CH_2
3	α 1.97 m β 1.50 [a]	37.1, CH_2	α 1.78 m β 1.24 m	31.6, CH_2
4	–	36.1, C	–	46.4, C
5	1.91 s	58.3, CH	–	73.0, C
6	3.92 br. s	65.1, CH	α 1.46 m β 1.69 [a]	32.6, CH_2
7	α 1.74 d (14.4) β 2.15 d (14.4)	34.2, CH_2	α 1.98 m β 1.69 [a]	32.3, CH_2
8	–	43.1, C	–	45.0, C
9	2.08 m	55.1, CH	1.63 [a]	48.3, CH
10	–	51.2, C	–	46.5, C
11	4.26 s	76.0, CH	α 1.36 m β 1.63 [a]	28.8, CH_2
12	2.49 s	50.5, CH	2.34 br. s	35.6, CH
13	4.28 s	71.4, CH	α 1.81 m β 1.49 m	44.3, CH_2
14	2.70 d (8.4)	50.1, CH	1.53 [a]	45.7, CH
15	α 2.16 m β 2.05 m	33.2, CH_2	5.28 d (0.8)	128.4, CH
16	–	143.6, C	–	151.6, C
17	a 4.89 s b 4.70 s	109.1, CH_2	2.27 m	33.2, CH_2
18	1.15 s	29.5, CH_3	1.05 s	19.3, CH_3
19	α 3.81 d (11.4) β 2.99 d (11.4)	60.0, CH_2	7.38 d (3.2)	172.8, CH
20	4.53 s	68.0, CH	3.48 br. s	81.4, CH
1′	α 1.63 m β 1.32 m	28.4, CH_2	α 1.79 [a] β 2.74 d (15.2)	34.0, CH_2
2′	α 2.07 m β 2.27 m	19.7, CH_2	4.14 [a]	67.8, CH
3′	α 1.20 m β 1.98 [a]	35.6, CH_2	α 1.51 m β 1.79 [a]	40.4, CH_2
4′	–	49.0, C	–	37.8, C
5′	1.54 m	53.7, CH	1.60 [a]	59.6, CH
6′	α 1.42 m β 1.98 m	21.9, CH_2	3.65 s	71.0, CH
7′	α 2.17 m β 2.03 m	33.7, CH_2	α 1.80 m β 1.71 m	40.6, CH_2
8′	–	42.3, C	–	40.5, C
9′	2.24 m	53.9, CH	1.60 [a]	59.6, CH
10′	–	53.7, C	–	46.4, C
11′	α 1.60 m β 2.06 m	30.4, CH_2	4.98 s	92.9, CH
12′	2.40 br. s	31.8, CH	5.65 d (6.4)	121.2,CH
13′	α 1.32 m β 1.64 m	35.9, CH_2	4.14 [a]	70.9, CH
14′	1.98 [a]	52.6, CH	1.75 m	48.8, CH
15′	5.63 s	128.0, CH	α 1.88 d (19.2) β 2.23 d (19.2)	37.4, CH_2
16′	–	146.3, C	–	145.8, C
17′	a 4.17 d (14.2) b 3.87 d (14.2)	68.8, CH_2	2.16 m	35.5, CH_2
18′	0.98 s	24.2, CH_3	0.99 s	30.0, CH_3
19′	9.85 s	206.7, CH	α 3.34 d (11.2) β 2.46 d (11.2)	64.3, CH_2
20′	–	227.3, C	3.30 m	66.4, CH

[a] indicates overlapping signals.

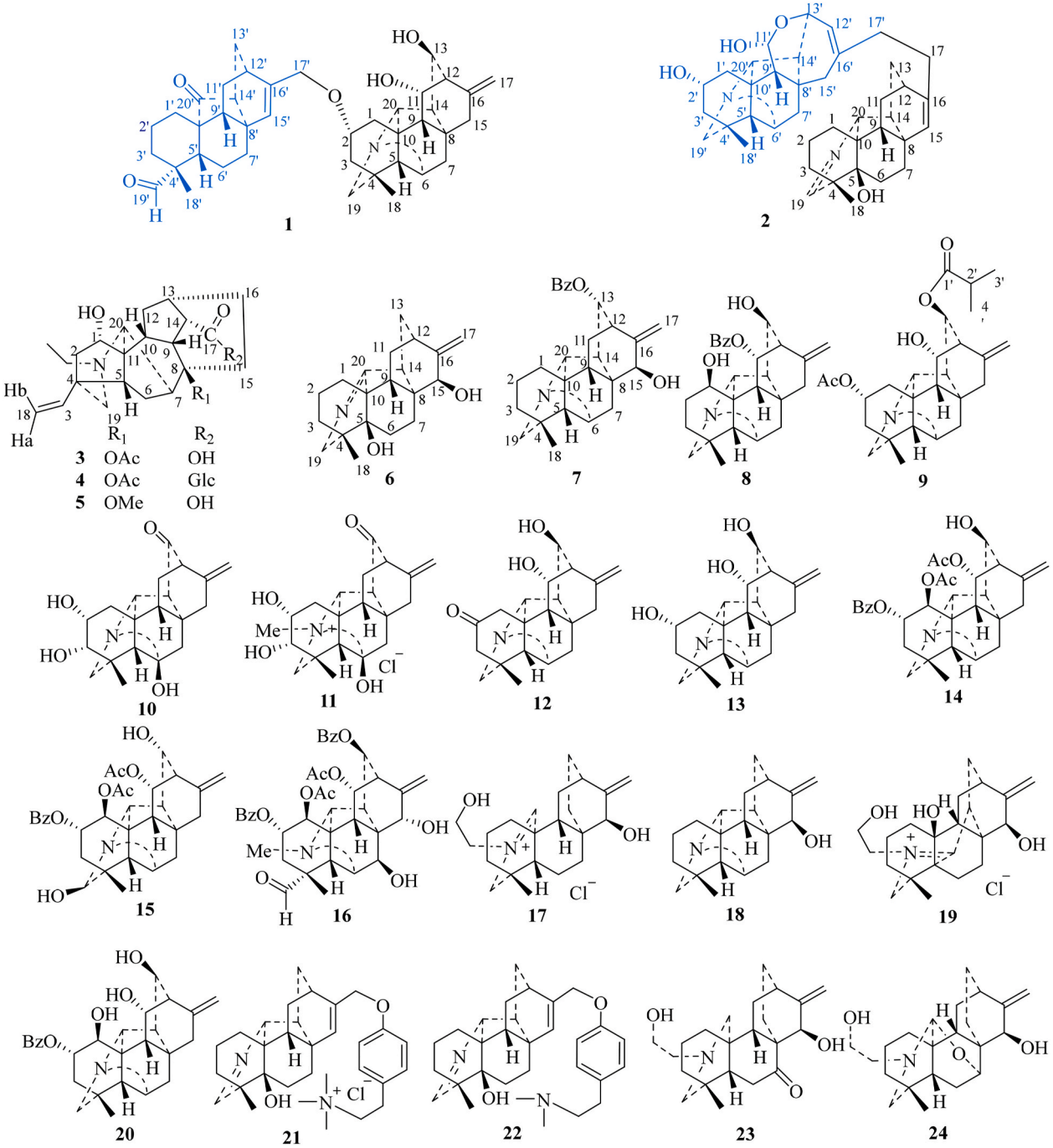

Fig. 1. Structures of compounds **1**–**24**.

The molecular formula of anthoroidine B (**2**), which was isolated as a white powder, was inferred to be $C_{40}H_{52}N_2O_4$ from its HRESIMS ($[M + H]^+$ at *m/z* 625.3997, calcd for $C_{40}H_{53}N_2O_4$: 625.4005) and ^{13}C NMR data. Analysis of its NMR data (Table 1) revealed the existence of two angular methyl groups [δ_H 1.05 (3H, s), 0.99 (3H, s); δ_C 19.3 (q), 30.0 (q)], two trisubstituted double bonds [δ_H 5.28 (1H, d, J = 0.8 Hz); δ_C 128.4 (d), 151.6 (s); δ_H 5.65 (1H, d, J = 6.4 Hz); δ_C 121.2 (d), 145.8 (s)], and two diagnostic sets of three non–oxygenated quaternary carbons (δ_C 46.4/37.8, 45.0/40.5, 46.5/46.4) and an oxygenated methylene carbon (δ_C 73.0). The aforementioned evidence suggested that compound **2** consisted of two C_{20}–diterpenoid alkaloid moieties (Wang and Liang, 2002). Comparison of the ^{13}C NMR, HMQC, and DEPT data with those of the known bis–diterpenoid alkaloid trichocarpinine (Lin et al., 2009) indicated that one moiety of **2** was connected to the hetidine–type moiety of trichocarpinine, which was further verified by 2D NMR experiments. Apart from the hetidine–type alkaloid skeleton, further comparison of the NMR data with those of the known compound hetisine (Jiang et al., 2012) indicated that they have the same molecular skeleton; the main differences were the hemiacetal group at C–11′ in **2**, and that the typical exocyclic double bond was isomerized to a C–12′–C–16′ endocyclic double bond. These changes were confirmed by the HMBC cross–peaks of H–11′/C–8′ and C–9′, and of H–12′/C–14′, C–16′ and C–17′, and the ^1H–^1H COSY correlations of H–11′/H–9′, and H–12′/H–13′. Furthermore, the hetidine–type alkaloid moiety (in black) was linked with the hetisine fragment (in blue) via a single bond between C–17′ and C–17 based on the HMBC correlations of H–17/C–16′ and C–17′ and of H–17′/C–16 and C–17 as well as the ^1H–^1H COSY correlation of H–17′/H–17.

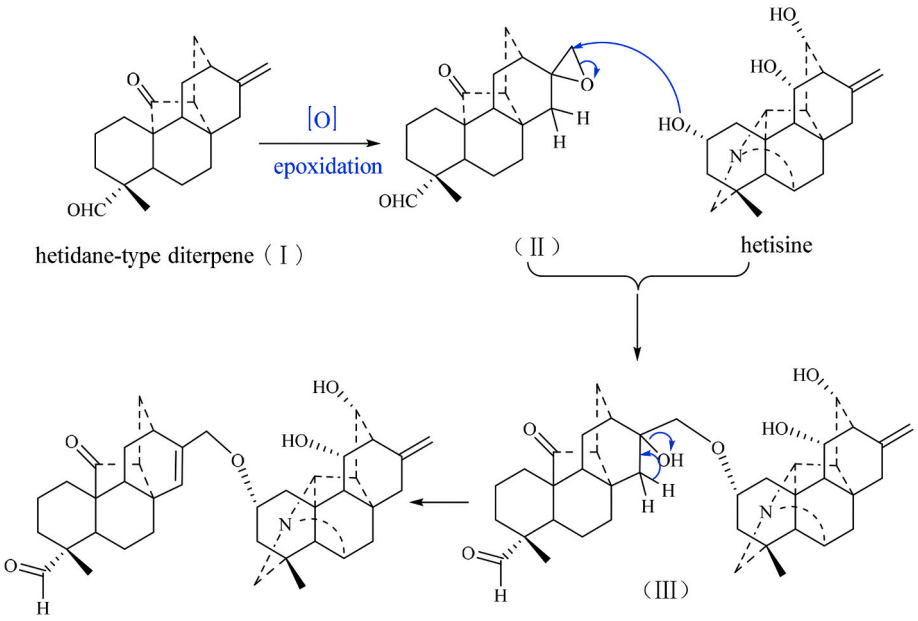

Fig. 2. Plausible biosynthetic pathway of anthoroidine a (**1**).

In the NOESY spectrum of **2** (Fig. S2), the cross–peak between H–1′*β*/H–13′, and H-11′/H-15′*β*, proved that H–11′ and H–13′ were β–oriented. Since the absolute configurations of hetitidine and hetisine were confirmed by X–ray crystallographic analysis (Tashkhodzhaev et al., 1992; Tang et al., 2008), the absolute configuration in **2** was proposed to be the same, which was further supported by comparison of its experimental and calculated electronic circular dichroism (ECD) spectra using the quantum chemical time-dependent density functionaltheory (TDDFT) method (Cheng et al., 2019) (Fig. S84). Hence, the structure of anthoroidine B (**2**) was determined as shown.

A possible biosynthetic pathway for **2** was proposed (Fig. 3), and two coexisting alkaloids, naviculine B (a) and guanfu base V (b), were considered to be the monomeric biosynthetic precursors of **2**. An intermolecular [2 + 2] cycloaddition of two diterpenoid alkaloids would give intermediate I, which could then be transformed into key intermediate III by oxidation and elimination to furnish the C–17′–C–17 single bond of **2**. Intermediate III would be finally converted to anthoroidine B by a retro–aldol followed by an intramolecular nucleophilic addition reaction of a hydroxyl group and a formyl group.

The molecular formula of compound **3** was determined to be $C_{24}H_{33}NO_5$ from its HRESIMS signal at *m/z* 416.2432 $[M + H]^+$ (calcd for $C_{24}H_{34}NO_5$, 416.2437). The IR data showed the presence of hydroxy groups (3353 cm^{-1}) and carbonyl groups (1716 cm^{-1}). The NMR data (Table 2) showed the presence of an *N*–ethyl group [δ_H 1.11 (3H, t, J = 7.2 Hz); δ_C 13.3 (q), 48.1 (t)], a methine carbon bearing a hydroxyl group [δ_H 3.88 (1H, d, J = 9.6 Hz); δ_C 75.3 (d)], an acetoxy group [δ_H 1.88 (3H, s), δ_C 22.5 (q), 170.0 (s)], a carboxyl group (δ_C 178.6) and a vinyl group [δ_H 5.61 (1H, dd, J = 18.0, 11.4 Hz), 4.88 (1H, d, J = 18.0 Hz), 4.96 (1H, d, J = 18.0 Hz); δ_C 141.9 (d), 113.1 (t)]. Further analyses of its ^{13}C NMR and DEPT spectra, which showed three diagnostic carbon signals of two quaternary carbons (δ_C 47.3 and 57.3) and one oxygenated tertiary carbon (δ_C 88.5), suggested that **3** had a rare C_{20}–diterpenoid alkaloid skeleton similar to that of racemulosine (Wang et al., 2000). Comparison of NMR data to racemulosine and HRESIMS,

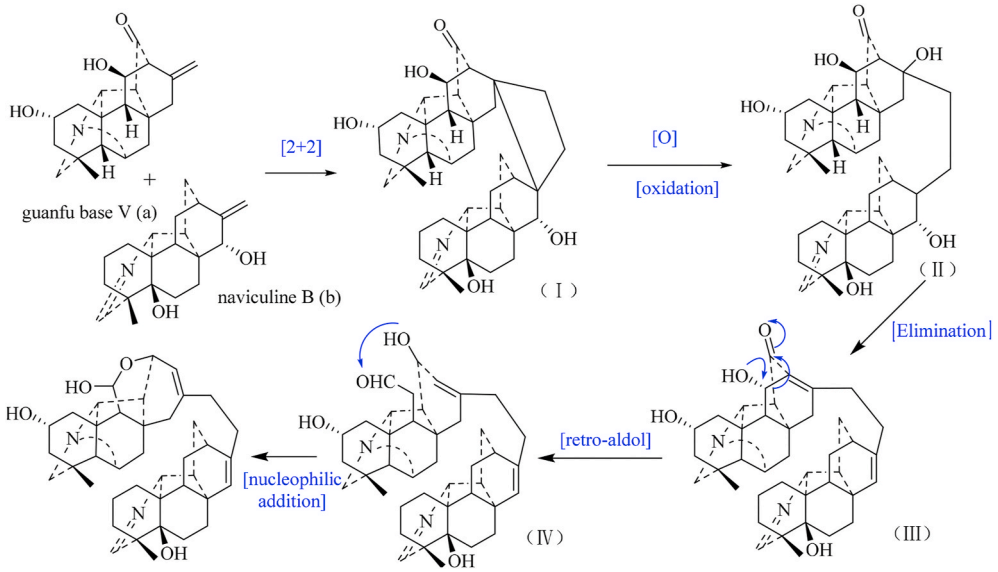

Fig. 3. Plausible biosynthetic pathway of anthoroidine B (**2**).

Table 2
NMR Data for Compounds **3**–**5** (^{1}H: 600 MHz,^{13}C: 150 MHz; δ in ppm, J in Hz; in $CDCl_3$).

No.	3		4		5	
	δ_H	δ_C, type	δ_H	δ_C, type	δ_H	δ_C, type
1	3.88 d (9.6)	75.3, CH	3.85 d (9.6)	75.3, CH	3.88 d (9.6)	75.3, CH
2	α 1.64 d (13.8) β 2.24 m	49.5, CH_2	α 1.64 d (13.8) β 2.23 m	49.5, CH_2	α 1.66 d (13.8) β 2.27 m	49.5, CH_2
3	5.61 dd (18.0, 11.4)	141.9, CH	5.62 dd (18.0, 11.4)	141.8, CH	5.65 dd (18.0, 11.4)	141.8, CH
4	–	47.3, C	–	47.2, C	–	57.4, C
5	1.94 d (7.2)	53.7, CH	1.90 [a]	53.5, CH	1.95 d (7.8)	53.4, CH
6	α 1.43 dd (15.0, 7.2) β 1.78 m	24.8, CH_2	α 1.41 m β 1.75 m	24.8, CH_2	α 1.42 dd (15.0, 7.2) β 1.81 dd (15.0, 7.2)	23.9, CH_2
7	3.28 d (7.2)	42.8, CH	3.21 d (6.6)	42.8, CH	2.53 d (7.2)	41.1, CH
8	–	88.5, C	–	88.4, C	–	82.4, C
9	2.66 dd (6.6, 4.8)	44.7, CH	2.66 t (6.0)	44.5, CH	2.34 [a]	42.6, CH
10	2.19 m	46.0, CH	2.18 m	45.8, CH	2.17 m	46.2, CH
11	–	57.3, C	–	57.2, C	–	57.4, C
12	α 1.75 m β 1.95 m	34.4, CH_2	α 1.76 m β 1.90 [a]	34.2, CH_2	α 1.76 m β 2.34 [a]	33.3, CH_2
13	2.47 m	32.6, CH	2.49 m	32.8, CH	2.71 m	35.6, CH
14	2.53 m	48.2, CH	2.63 m	48.1, CH	2.73 m	50.8, CH
15	α 1.79 m β 2.45 m	29.4, CH_2	α 1.86 m β 2.43 m	29.0, CH_2	α 1.82 m β 2.38 m	26.3, CH_2
16	α 1.27 m β 2.23 m	28.1, CH_2	α 1.28 m β 2.15 m	28.1, CH_2	α 1.26 m β 2.26 m	26.7, CH_2
17	–	178.6, C	–	171.9, C	–	174.0, C
18	a 4.96 br. d (11.4) b 4.88 br. d (18.0)	113.1, CH_2	a 4.97 br. d (11.4) b 4.88 br. d (18.0)	113.1, CH_2	a 5.00 br. d (11.4) b 4.91 br. d (18.0)	113.1, CH_2
19	α 2.31 d (10.8) β 2.57 [a]	55.5, CH_2	α 2.30 d (10.8) β 2.59 m	55.4, CH_2	α 2.63 d (10.8)	55.6, CH_2
20	2.98 s	62.4, CH	2.97 s	62.4, CH	2.96 s	62.5, CH
21	a 2.54 m b 2.52 m	48.1, CH_2	a 2.55 m b 2.52 m	48.1, CH_2	a 2.57 m b 2.54 m	48.1, CH_2
22	1.11 t (7.2)	13.3, CH_3	1.12 t (7.2)	13.3, CH_3	1.14 t (7.2)	13.3, CH_3
OAc	1.88 s	22.5, CH_3 170.0, C	1.93 s	22.7, CH_3 170.9, C		
OMe					3.22 s	48.6, CH_3
1′			5.58 d (7.8)	94.1, CH		
2′			3.48 m	72.9, CH		
3′			3.59 m	76.8, CH		
4′			3.56 m	69.9, CH		
5′			3.46 m	76.6, CH		
6′			3.79 br s	61.6, CH_2		

[a] indicates overlapping signals.

the major differences included 3 bearing an acetoxy group at C-8 instead of a hydroxyl group, and the $CONH_2$ group (δ_C 179.5) at C-14 replaced by a COOH group (δ_C 178.6) in racemulosine. The carbon signal of C–8 at (δ_C 70.6) in racemulosine was shifted downfield to (δ_C 88.5) in compound **3**, suggesting that the acetoxy group in **3** might be located at C–8, and which was further confirmed by the HMBC correlations from H–6/H–7/H–9/H–14 to C–8. In addition, the carboxyl group was located at C–14 base on the HMBC correlations from H–14 to C–17 and the molecular formula deduced from HRESIMS.

The relative configuration of compound **3** (Fig. S2) was deduced from a NOESY experiment. The NOESY cross–peaks between H–1/H–5, H–1/H–10 indicated the α–orientation of OH–1. Additionally, the cross–peak between H–14/H–10 showed that H–14 is *β*–oriented. Since the absolute configuration of the skeleton of racemulosine was confirmed by X–ray crystallography (Wang et al., 2000), the absolute configuration of this skeleton was proposed to be retained in **3**. Therefore, the structure and absolute configuration of anthoroisine C (**3**) were defined as shown in Fig. 1.

The HRESIMS signal at m/z 578.2968 $[M + H]^+$ (calcd for $C_{30}H_{44}NO_{10}$, 578.2965) implied that the molecular formula of **4** was $C_{30}H_{43}NO_{10}$. A comparison of the ^{13}C NMR data of **3** and **4** indicated the presence of resonances for a sugar moiety (δ_C 94.1, 76.8, 76.6, 72.9, 69.9 and 61.7) (Huang et al., 2013), which was identified as *β–D–*glucose by gas chromatography of the hydrolyzed product (Fig. S39) and based on the coupling constant of the anomeric proton [δ_H 5.58 (1H, d, $J = 7.8$ Hz)]. Relative to those of **3**, the ^{13}C NMR signal of C–17 of **4** was shifted upfield ($\Delta\delta_C$ 6.7 ppm), suggesting that the glucose moiety was located at C–17, which was supported by the HMBC correlation of H–1′ with C–17. All of the available evidence suggests that the structure of anthoroisine D (**4**) is as depicted in Fig. 1.

The protonated molecular ion in the HRESIMS data of compound **5** at m/z 388.2482 (calcd for $C_{23}H_{34}NO_4$: 388.2488, $[M + H]^+$) provided a molecular formula of $C_{23}H_{33}NO_4$. Combined analyses of the spectroscopic data suggested that **5** is structurally similar to **3**, indicated that **5** also possesses a racemulosine–type diterpenoid alkaloid skeleton, the main difference was that the acetoxy at C–8 in **3** was replaced by a methoxy group in **5**, which was validated by the loss of 28 mass units in mass spectrometry. This replacement was supported by the HMBC correlations (Fig. S1) of the protons of OCH_3–8 with C–8. Thus, the structure of anthoroisine E (**5**) was confirmed by extensive analyses of its 1D and 2D NMR spectra.

Compound **6** possessed the molecular formula $C_{20}H_{27}NO_2$, which was determined from its HRESIMS signals at m/z 314.2114 ($[M + H]^+$, calcd 314.2120). **6** was determined to be a hetidine–type C_{20}–diterpenoid alkaloid based on its NMR spectra (Tables 3 and 4), which showed the presence of an exocyclic double bond [(δ_H 4.99 (s) and 5.02 (s); δ_C 156.3 (s), 109.1 (t)], a methyl group [δ_H 0.92 (s); δ_C 21.6 (q)], and three diagnostic non–oxygenated quaternary carbon signals (δ_C 38.9, 45.2, and 50.2) (Wang and Liang, 2002). The signal at δ_C 183.6 in the ^{13}C NMR data indicated that C–20 is connected to a nitrogen through a double bond (Wang and Liang, 2002), which was supported by the HMBC correlations of H–1, H–9, and H–19 with C–20. Along with the above–mentioned signals, the ^{13}C NMR spectrum of **6** displayed signals for two oxygenated carbons [δ_C 77.0 (s) and 71.5 (d)], suggesting that this compound possessed two additional hydroxy groups. These two hydroxy groups were assigned at C–5 and C–15 based on the HMBC correlations from H–6, H–7, H–18, and H–19 to C–5 and from H–9 and H–17 to C–15. In the NOESY spectrum of **6**, the cross–peak between H–15 and H–7α, H–7α and H–14 proved that H–15 was α–oriented. Therefore, the structure of anthoroisine F (**6**) was determined as shown in Fig. 1, and the full assignment of its spectroscopic data was achieved based on the 1D–and 2D NMR analysis.

The molecular formula of compound **7** was established as $C_{27}H_{31}NO_3$ based on its HRESIMS and ^{13}C NMR data. NMR spectroscopic data (Tables 3 and 4) of compound **7** in conjunction with the HSQC data indicated the presence of an angular methyl group [δ_H 0.97 (3H, s); δ_C

Table 3
^{1}H NMR Data for Compounds **6**–**9** (600 MHz, in $CDCl_3$, δ_H in ppm, J in Hz).

No.	6	7	8	9
1	α 1.89 m β 1.42 m	α 1.84 m β 1.20 m	4.07 [a]	α 1.94 d (16.2) β 2.95 d (16.2)
2	α 1.44 m β 1.63 m	α 1.47 m β 1.64 m	α 3.13 d (14.4) β 1.40 m	a 5.19 m
3	α 1.71 m β 1.13 m	α 1.44 m β 1.24 m	α 2.19 [a] β 1.37 m	α 1.54 dd (15.6, 4.2) β 1.84 br. d (15.6)
5	–	1.44 s	1.94 s	1.60 s
6	α 1.81 m β 1.72 m	3.22 br. s	3.89 br. s	3.22 s
7	α 1.32 dt (9.6, 1.2) β 2.35 [a]	α 1.70 dd (13.6, 2.8) β 2.09 dd (13.6, 2.8)	α1.85 dd (15.0, 7.8) β 2.15 m	α 1.75 dd (15.6, 2.4) β 1.62 dd (15.6, 2.4)
9	2.32 m	1.84 [a]	2.44 m	1.98 dd (10.2, 2.4)
11	α 1.75 m β 2.03 dd (14.4, 4.2)	α 1.62 m β 1.93 dd (14.4, 4.0)	5.47 d (9.0)	a 4.28 d (9.0)
12	2.34 m	2.55 m	2.68 d (2.4)	2.43 d (2.4)
13	α 1.72 [a] β 1.41 m	4.56 d (2.4)	4.30 d (9.0)	5.15 dt (10.2, 2.4)
14	2.25 d (10.2)	1.84 [a]	3.03 d (9.0)	2.28 dd (10.2, 2.4)
15	4.03 s	4.10 s	α 2.19 [a] β 2.42 m	α 2.22 d (17.4) β 2.04 d (17.4)
17	a 5.02 s b 4.99 s	a 5.18 s b 5.03 s	a 4.99 s b 4.82 s	a 4.91 s b 4.72 s
18	0.92 s	0.97 s	1.11 s	0.98 s
19	α 3.79 ABq (19.2) β 3.56 ABq (19.2)	α 2.43 ABq (12.4) β 2.51 ABq (12.4)	α 4.09 ABq (12.0) β 2.99 ABq (12.0)	α 2.86 ABq (12.0) β 2.50 ABq (12.0)
20		2.87 s	4.78 s	3.46 s
2′				2.51 m
3′		7.94 d (7.6)	8.15 d (7.2)	1.18 q (6.6)
4′		7.39 t (7.6)	7.44 t (7.8)	1.16 q (6.6)
5′		7.52 t (7.6)	7.56 t (7.8)	
6′		7.39 t (7.6)	7.44 t (7.8)	
7′		7.94 d (7.6)	8.15 d (7.2)	
OAc				2.03 (s)

[a] indicates overlapping signals.

Table 4
^{13}C NMR Data for Compounds **6**–**9** (150 MHz, in $CDCl_3$, δ_C in ppm).

No.	6	7	8	9
1	26.7, CH_2	26.4, CH_2	65.9, CH	31.4, CH_2
2	20.2, CH_2	19.7, CH_2	31.2, CH_2	70.4, CH
3	35.0, CH_2	34.0, CH_2	38.0, CH_2	36.7, CH_2
4	38.9, C	38.1, C	35.6, C	36.7, C
5	77.0, C	61.1, CH	58.0, CH	61.5, CH
6	27.3, CH_2	65.2, CH	65.0, CH	64.3, CH
7	30.6, CH_2	32.4, CH_2	34.3, CH_2	36.3, CH_2
8	45.2, C	46.1, C	43.5, C	44.1, C
9	51.3, CH	43.1, CH	53.3, CH	55.4, CH
10	50.2, C	49.8, C	50.4, C	50.7, C
11	26.3, CH_2	23.3, CH_2	75.9, CH	75.5, CH
12	33.8, CH	38.5, CH	47.9, CH	48.8, CH
13	31.0, CH_2	76.3, CH	70.2, CH	74.0, CH
14	36.2, CH	52.9, CH	50.4, CH	50.4, CH
15	71.5, CH	71.3, CH	33.1, CH_2	34.0, CH_2
16	156.3, C	150.6, C	143.6, C	144.9, C
17	109.1, CH_2	112.8, CH_2	109.8, CH_2	108.9, CH_2
18	21.6, CH_3	28.9, CH_3	29.4, CH_3	29.7, CH_3
19	65.0, CH_2	63.0, CH_2	60.4, CH_2	63.5, CH_2
20	183.6, C	72.0, CH	68.7, CH	68.9, CH
1′		166.0, C	166.8, C	176.5, C
2′		130.5, C	130.1, C	34.0, CH
3′		129.6, CH	128.7, CH	19.6, CH_3
4′		128.4, CH	130.3, CH	18.9, CH_3
5′		133.0, CH	133.4, CH	
6′		128.4, CH	130.3, CH	
7′		129.6, CH	128.7, CH	
OAc				170.3, C
				22.0, CH_3

28.9], six methylenes (δ_C 26.4, 19.7, 34.0, 32.4, 23.3, 63.0), eight sp^3 methines (δ_C 61.1, 65.2, 43.1, 38.5, 76.3, 52.9, 71.3, 72.0), and three sp^3 quaternary carbons (δ_C 38.1, 46.1, 49.8), one exocyclic methylene group [δ_H 5.03 (br. S) and 5.18 (br. S); δ_C 112.8, 150.6], and a benzoyl group [δ_H 7.94 (2H, d, J = 7.6 Hz), δ_H 7.52 (1H, t, J = 7.6 Hz), δ_H 7.39 (2H, t, J = 7.6 Hz); δ_C 130.5, 129.6 × 2, 128.4 × 2, 133.0, 166.0]. From the above–mentioned spectroscopic data, compound **7** could be assigned as a hetisine–type C_{20}–diterpenoid alkaloid possessing a benzoyl group (Wangchuk et al., 2007). Comparison of the 1D NMR data (Tables 3 and 4) of **7** with those of the known compound nominine (**18**) indicated that **7** has an additional benzoyl group located at C–13 and the HMBC cross–peaks between H–13 (δ_H 4.56, d, J = 2.4 Hz) and the carbonyl carbon (δ_C 166.0). The presence of a hydroxy group at C–15 was supported by the HMBC correlations from H–7 and H–9 to C–15 and from H–15 to C–16 and C–17, and these correlations are listed in Fig. S1. As shown in Fig. S2, the key NOESY correlations of H–13 with H–20, H–14 with H–15, and H–15 with H–7α indicated the β–orientation of H–13 and the α–orientation of H–15. The relative configuration of **7** was deduced base on analysis of the coupling constants, NOESY experiments (Fig. S2) and X–ray (Fig. 4) experiments. Therefore, the structure of anthoroisine G (**7**) was defined as shown in Fig. 1.

The HRESIMS data of **8** implied a molecular formula of $C_{27}H_{31}NO_4$ based on the signal at m/z 434.2326 ($[M + H]^+$, $C_{27}H_{32}NO_4$, calcd 434.2331). The NMR spectroscopic data strongly suggested that **8** was also a hetisine–type C_{20}–diterpenoid alkaloid bearing a benzoyl moiety and two hydroxy groups. Two hydroxy groups were assigned at C–1 (δ_C 65.9 d) and C–13 (δ_C 70.2 d) based on the HMBC correlations of H–3 and H–20 with C–1 and of H–11 and H–14 with C–13, respectively. Additionally, the location of the benzoyl group was established based on the HMBC correlation between H–11 and the carbonyl carbon (δ_C 166.8). The large coupling constant of H–13 (J = 9.0 Hz) with H–14α revealed that H–13 was in an α–orientation. In the NOESY experiment, the cross–peaks of H–1/H–20 suggested the α–orientation of H–1. The coupling constant between H–11 with H–9β (J = 9.0 Hz) indicated a 1,2-diaxial relationship between them, implying that H–11 was β-oriented, further supported by the correlations between H-11 and H–9β in the NOESY experiment. Consequently, all of the available evidence suggested the structure of anthoroisine H (**8**) is as depicted in Fig. 1.

Compound **9** was obtained as a white powder and had a formula of $C_{26}H_{35}NO_5$ as determined from its HRESIMS (m/z 442.2590 $[M + H]^+$, calcd 442.2593) and ^{13}C NMR spectra. The characteristic NMR spectroscopic data (Tables 3 and 4) of **9** strongly indicated that it was a hetisine–type C_{20}–diterpenoid alkaloid possessing a hydroxy group, an acetyl group [δ_H 2.03 (3H, s); δ_C 22.0 (q), 170.3 s)] and an isobutyryl group [δ_H 1.16 (3H, q, J = 6.6 Hz), 1.18 (3H, q, J = 6.6 Hz); δ_C 18.9 (q), 19.6 (q), 34.0 (d), 176.5 (s)]. Long–range correlations observed in the HMBC data from H–13 to the carbonyl carbon of the isobutyryloxy group indicated that the isobutyryloxy group was at C–13. Further analysis of the NMR spectra of **9** indicated that it was structurally related to the known alkaloid trichodelphinine D (Tang et al., 2008). The difference was that the acetyl group in trichodelphinine D was replaced by an isobutyryl group in **9**, which was also supported by 2D NMR and HRESIMS data. The large coupling constant in the ^{1}H NMR spectrum of **9** of H–13 (J = 10.2 Hz) with H–14α revealed that H–13 was in an α–orientation. The coupling constant of H–2 (J = 4.2 Hz) with H–3 indicated that H–2 was in an equatorial position, which indicated a β-orientation. Additionally, the coupling constant between H–11 with H–9β (J = 9.0 Hz) implying that H–11 was β-oriented. Hence, the structure of anthoroisine I (**9**) was confirmed as shown in Fig. 1.

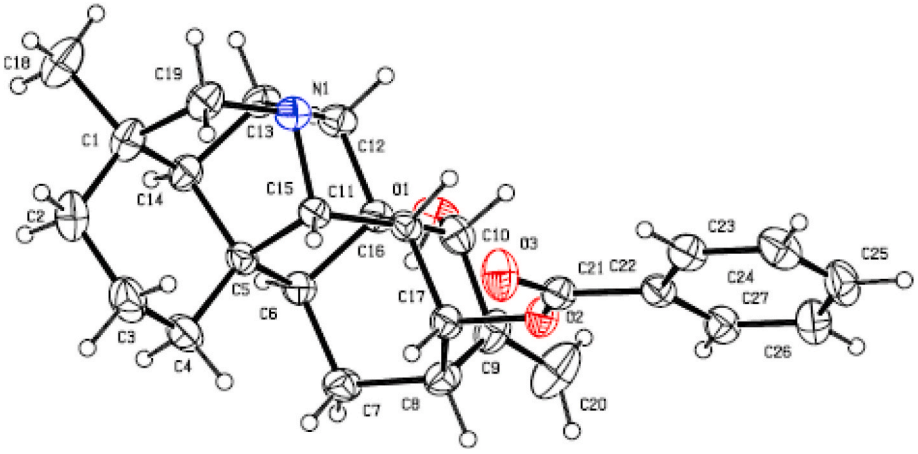

Fig. 4. ORTEP drawing of **7**.

2.2. Biological evaluation

1–Methyl–4–phenylpyridinium (MPP^+) is widely used as a neurotoxin for inducing a syndrome closely resembling classic PD in animal and cellular models (Singer and Ramsay, 1990; Przedborski and Jackson–Lewis, 1998). In this study, the effects of compounds **3**, **4**, and **6**–**19** on the viability of SH–SY5Y cells were determined by an MTT assay. Treatment with compounds **6**, **8**–**12**, **14**, and **17**–**19** resulted in more than 95% cell viability at 50 μM in the SH–SY5Y cell line (Table 5). Therefore, these compounds were chosen as candidate compounds for testing against MPP^+–induced cytotoxicity in SH–SY5Y cells (Table 6). Nominine (**18**) showed significant recovery of 34.4% at a concentration of 50 μM, while aconicarmicharcutinium A hydrochloride (**19**) showed the strongest recovery ratio of 16.8% at a concentration of 20 μM, and it was more potent than compounds **17, 18,** and **14**.

3. Conclusions

Although the etiologies of AD and PD are unknown, decreased acetylcholine levels are correlated with these progressive NDs (Bartus et al., 1982; Giacobine and Becker, 1997; Giacobini, 2000). The inhibition of AChE has thus been considered a promising approach for the treatment of AD and PD (Zhang et al., 2015). In our search for novel, potent cholinesterase inhibitors, compounds **3** and **6**–**24** (>5 mg of each of these compounds was obtained) were assayed *in vitro* for their inhibitory activity toward AChE, and huperzine A was employed as a positive control (Table 7). Rotundifosine F (**21**) showed the strongest AChEI activity (IC_{50} = 0.3 μM). Compounds **22** and **17** also displayed high potencies (IC_{50} < 2 μM), followed by **7**, **14**, **24**, **9**, and **23** (IC_{50} < 10 μM). The remaining alkaloids were inactive against AChE (IC_{50} > 10 μM). Based on the aforementioned biological data, the structure–activity relationships (SARs) for these diterpenoid alkaloids can be briefly summarized. (1) C–17 side-chain modifications might be an important factor for the activity of the hetidine–type diterpenoid alkaloids (compare **21**, **22** and **6**). (2) For hetisine–type diterpenoid alkaloids, the hydroxyl substituents at C–2 and C–19 are beneficial to the activity. (3) A benzoyl substituent at C–13 of hetisine–type alkaloids also improve the activity.

In summary, nine undescribed and ten known diterpenoid alkaloids

Table 5
Effects of compounds **3**, **4**, and **6**–**19** on the viability of SH–SY5Y cells [a].

Compound	Cell viability (%) [b] (20 μM)	Cell viability (%) [b] (50 μM)
3	91.2	84.3
4	86.4	90.2
6	111.4	99.0
7	89.0	64.0
8	104.6	104.0
9	103.9	98.3
10	102.2	100.6
11	104.5	106.7
12	107.9	99.6
13	83.0	84.5
14	94.9	101.5
15	89.3	71.5
16	92.8	75.6
17	99.0	98.7
18	104.2	98.1
19	108.8	95.3

[a] Inhibition rate = $(A_{490,\ control}–A_{490,\ sample})/(A_{490,\ control}–A_{490,\ blank}) \times 100$; Cell viability = 100– Inhibition rate.
[b] Mean value of three independent determinations.

Table 6
Effects of compounds **6**, **8**–**12**, **14,** and **15**–**17** against MPP^+–induced cytotoxicity in SH–SY5Y cells [a].

Compound	Recovery ratio (%) [b] (20 μM)	Recovery ratio (%) [b] (50 μM)
6	−10.2	−16.7
8	−11.5	−9.7
9	−37.4	−14.5
10	−6.4	−10.9
11	−7.5	−4.5
12	−4.1	−12.2
14	2.9	−6.8
17	13.6	14.9
18	5.1	34.4
19	16.8	7.8

[a] Recovery rate = $[(\text{cell viability})^+_{MPP+compound} - (\text{cell viability})^+_{MPP}]/[(\text{cell viability})^+_{MPP}] \times 100\%$.
[b] Mean value of three independent determinations.

Table 7
AChE inhibitory activities of compounds **3** and **6**–**24**.

Compound	IC_{50} (μM) ± S.E.M	Compound	IC_{50} (μM) ± S.E.M
3	27.4 ± 5.2	**15**	17.8 ± 9.2
6	17.6 ± 2.7	**16**	>50
7	6.3 ± 1.6	**17**	2.3 ± 0.2
8	>100	**18**	15.8 ± 1.7
9	9.3 ± 3.0	**19**	13.6 ± 2.4
10	20.4 ± 7.8	**20**	21.3 ± 9.2
11	>50	**21**	0.3 ± 0.02
12	17.7 ± 1.2	**22**	1.7 ± 0.6
13	8.4 ± 0.8	**23**	9.7 ± 3.8
14	6.4 ± 1.2	**24**	8.9 ± 4.9
huperzine A	0.065 ± 0.001		

[a] The treatments were replicated three times.

were isolated from the herb *A. anthoroideum* for the first time. More than 1500 natural diterpenoid alkaloids have been identified to date (Wang et al., 2010; McKay et al., 2007). In most cases, C_{20}–diterpenoid alkaloids contain only common groups, such as OH, OAc, OBz, and OCn (Wang and Liang, 2002). Compound **1** was the first example of a diterpenoid alkaloid conjugated to a unique diterpenoid moiety. To the best of our knowledge, approximately twenty naturally occurring bis-diterpenoid alkaloids have been reported, and in all the reported bis-diterpenoid alkaloids, the two diterpenoid alkaloid moieties were linked with an O–ether linkage (Wang and Liang, 2002; Lin et al., 2009; Zhang et al., 2013; Cai et al., 2010; Duan et al., 2019; He et al., 2017; Ding et al., 1992). Compound **2** is the first bisditerpenoid alkaloid joined with a C–17′–C–17 single bond. Interestingly, the racemulosine–type diterpenoid alkaloid is a rare C_{20}–diterpenoid alkaloid with a unique skeleton, and it was proposed to originate from a denudatine–type diterpenoid alkaloid through double Wanger–Meerwein rearrangements of rings A and C (Wang and Liang, 2002). To date, racemulosine, isolated from *A. racemulosum Franch* var. *Pengzhouense*, is the only member of this subclass (Wang et al., 2000). Excitingly, three racemulosine–type C_{20}–diterpenoid alkaloids, anthoroidines C–E (**3**–**5**), were isolated from *A anthoroideum* DC., which may serve as a reliable taxonomic marker of the subgenus Aconitum. Glucose is ubiquitous in plants; however, only five diterpene alkaloids containing a glucose moiety have been reported to date (Zhang et al., 2016; Meng et al., 2017a,b). Compound **4** is the first diterpenoid alkaloid with a racemulosine skeleton bearing a glucose isolated from a natural source, providing a new candidate for further pharmacological investigations. To the best of our knowledge, aconicarmicharcutinium hydrochloride is the only arcutine–type C_{20}–diterpenoid alkaloid with an iminium moiety, and its absolute configuration has been unambiguously established by X–ray crystallographic analysis (Fig. 5) for the first time in this report. In addition, the assay of the neuroprotective effects indicated for the first time that some of these isolated compounds could protect SH–SY5Y cells from MPP^+–induced apoptosis and increase cell viability. Nominine (**18**) showed a highly potent protective effect, with a recovery rate of 34.4% (50 μM). The AChE inhibitory activities of these compounds as well as five known diterpenoid alkaloids were also assessed. Rotundifosine F (**21**) exhibited significantly higher AChE inhibitory activity relative to those of other alkaloids, suggesting its potential as a new lead compound for the development of AChE inhibitors. The phytochemical investigation, bioactivity examination, and SAR analysis of these diterpenoid alkaloids in the current study not only enriches the chemical diversity of diterpenoid alkaloids but also contributes to the development of potential ND therapeutic drugs.

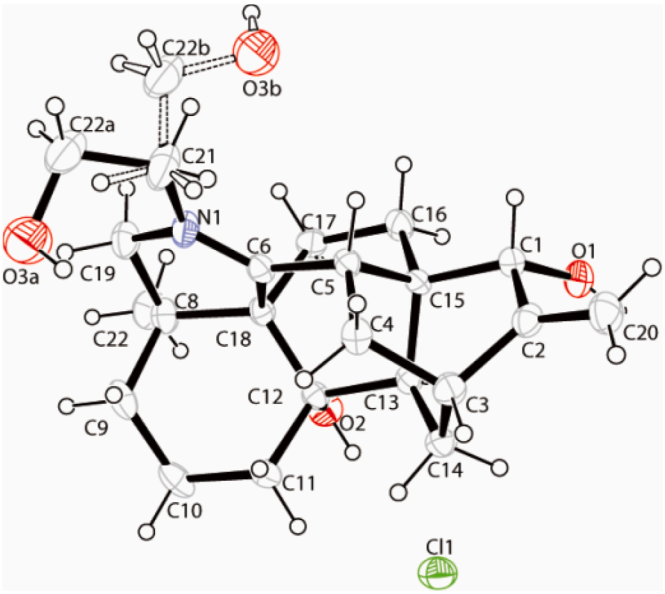

Fig. 5. ORTEP drawing of **19**.

4. Experimental section

4.1. General experimental procedures

Optical rotations were determined using a PerkinElmer polarimeter with a sodium lamp operating at 598 nm and 20 °C. IR spectra were obtained using a Thermo Fisher Nicolet 6700 spectrometer. The NMR spectra were recorded on a Bruker AV 600 spectrometer. HRESIMS data were measured using a Q–TOF micro mass spectrometer (Waters). HPLC separations were carried out on a Waters SymmetryShield™ RP–18 column (5 μm, 4.6 × 250 mm) with a Waters 600 controller and a Waters 2487 detector.

ECD spectra were measured on an Aviv Model 420SF spectropolarimeter (Aviv Biomedical Inc., Lakewood, USA). Silica gel (Qingdao Haiyang Chemical Co., Ltd., China) and Sephadex LH–20 (Pharmacia Co.) were utilized for column chromatography (CC).

4.2. Plant material

The whole plants of *A. anthoroideum* DC. (Ranunculaceae) were collected in August 2016 from Sayram Lake, Bortala, Xinjiang, People's Republic of China (GPS coordinates: 44°64′N, 81°38′E). The plant was identified by Professor Liangke Song of the School of Life Science and Engineering, Southwest Jiaotong University, Sichuan, P. R. China, and a voucher specimen was deposited at the same institution (*No.* ZN361520160816).

4.3. Extraction and isolation

Air–dried whole plants of *A. anthoroideum* DC. (4.8 kg) were extracted with 95% EtOH five times at room temperature, and each extraction lasting four days. The solvent was evaporated to afford the ethanol extract (500 g). The extract was suspended in H_2O (2 L) and adjusted to pH 2–3 with 10% HCl and sequentially extracted with petroleum ether (3 × 3 L) and ethyl acetate (3 × 3 L). The pH of the aqueous layer was adjusted to 11 with aqueous ammonia solution, and it was extracted with CH_2Cl_2 (3 × 3 L). The CH_2Cl_2 extracts were concentrated to produce the crude alkaloid extract (18 g). The crude alkaloid extract was separated by column chromatography over silica gel using CH_2Cl_2:MeOH (100:1–1:100) mixtures with increasing polarity, and fractions A–E were obtained based on TLC analysis.

Fr. A (3.2 g) was subjected to a silica gel column with light petroleum:acetone:Et_2NH (25:1:0.1–0:1:0.1) to obtain compounds **3** (20 mg), **5** (2 mg), and **9** (10 mg). Fr. B (2.8 g) was submitted to silica gel CC eluting with light petroleum:acetone:Et_2NH (20:1:0.1–0:1:0.1) to yield compounds **6** (16 mg), **7** (60 mg), and **14** (15 mg). Fr. C (4 g) was separated on a silica gel column (light petroleum:acetone:Et_2NH, 18:1:0.1–0:1:0.1) to afford subfractions C_1 (80 mg), C_2 (200 mg), C_3 (480 mg), C_4 (230 mg), and C_5 (150 mg). Subfractions C_1 and C_2 were separated on silica gel (light petroleum:acetone:Et_2NH, 16:1:0.1–0:1:0.1) to afford compounds **8** (11 mg), **13** (9.2 mg) and **15** (15 mg). Compounds **12** (24 mg), **16** (9 mg), **17** (12 mg), and **18** (17 mg) were obtained by purifying subfraction C_3 by silica gel CC (light petroleum:acetone:Et_2NH, 13:1:0.1–0:1:0.1). Fr. D (2 g) was subjected to silica gel CC and eluted with CH_2Cl_2:MeOH (40:1–1:1) to obtain four subfractions (D_1–D_3). Subfraction D_2 was subjected to Sephadex LH–20 column chromatography (MeOH) to yield compound **9** (8 mg). Subfraction D_3 was further purified using an RP–18 silica gel column with MeOH:H_2O (15:85–50:50) as the mobile phase to yield compounds **4** (5 mg) and **16** (45 mg) and a mixture (23 mg) that was further purified over RP–18 silica gel with MeOH:H_2O (3:7) to afford compounds **1** (2 mg) and **2** (2 mg). Compounds **11** (13 mg), **10** (13 mg), and **19** (19 mg) were

isolated from fraction E (258 mg) with mixtures of light petroleum: acetone:Et_2NH of 9:1:0.1, 8:1:0.1 and 4:1:0.1, respectively.

4.3.1. Anthoroisine A (1)

White powder; [α]20 D = −4.5 (*c* 0.35, $CHCl_3$); IR (KBr) ν_{max}: 3393, 3349, 2919, 2850, 1723, 1666, 1460, 1384, 1084, 1047, 884, 600 cm^{-1}; ^1H NMR and ^{13}C NMR data, see Table 1. HRESIMS (*m/z*): 626.3845 $[M + H]^+$ (calcd For $C_{40}H_{52}NO_5$: 626.3845).

4.3.2. Anthoroisine B (2)

White powder; [α]20 D = +37.2 (*c* 0.5, CH_3OH); IR (KBr) ν_{max}: 3399, 2926, 2870, 1644, 1457, 1368, 1344, 1315, 1180, 1080, 1025 cm^{-1}; ^1H NMR and ^{13}C NMR data, see Table 1. HRESIMS (*m/z*): 625.3997 $[M + H]^+$ (calcd for $C_{40}H_{53}N_2O_4$: 625.4005).

4.3.3. Anthoroisine C (3)

White powder; [α]20 D +27.0 (*c* 0.5, $CHCl_3$); IR (KBr) ν_{max} 3353, 3074, 2937, 2875, 1716, 1562, 1397, 1255, 1190, 1147, 1038, 999, 755 cm^{-1}; ^1H NMR and ^{13}C NMR data, see Table 2; HRESIMS *m/z* 416.2432 $[M + H]^+$ (calcd for $C_{24}H_{34}NO_5$: 416.2437).

4.3.4. Anthoroisine D (4)

White powder; [α]20 D +10.6 (*c* 0.5, $CHCl_3$); IR (KBr) ν_{max} 3369, 2925, 2875, 1727, 1568, 1459, 1416, 1372, 1256, 1073, 1034, 964, 757 cm^{-1}; ^1H NMR and ^{13}C NMR data, see Table 2; HRESIMS *m/z* 578.2968 $[M + H]^+$ (calcd for $C_{30}H_{44}NO_{10}$: 578.2965).

4.3.5. Anthoroisine E (5)

White powder; [α]20 D +50.0 (*c* 0.1, $CHCl_3$); ^1H NMR and ^{13}C NMR data, see Table 2; HRESIMS *m/z* 388.2482 $[M + H]^+$ (calcd for $C_{23}H_{34}NO_4$: 388.2488).

4.3.6. Anthoroisine F (6)

White powder; [α]20 D +68.2 (*c* 0.45, $CHCl_3$); IR (KBr) ν_{max} 3358, 2961, 2932, 1663, 1460, 1260, 1135, 1093, 897, 803 cm^{-1}; ^1H NMR and ^{13}C NMR data, see Tables 3 and 4; HRESIMS *m/z* 314.2114 $[M + H]^+$ (calcd for $C_{20}H_{28}NO_2$: 314.2120).

4.3.7. Anthoroisine G (7)

White powder; [α]20 D +19.0 (*c* 0.50, $CHCl_3$); IR (KBr) ν_{max} 3405, 3071, 2949, 2923, 1717, 1450, 1278, 1448, 1263, 1112, 1071, 748, 714 cm^{-1}; ^1H NMR and ^{13}C NMR data, see Tables 3 and 4; HRESIMS *m/z* 418.2379 $[M + H]^+$ (calcd for $C_{27}H_{32}NO_3$: 418.2382).

4.3.8. Anthoroisine H (8)

White powder; [α]20 D +15.5 (*c* 0.18, $CHCl_3$); IR (KBr) ν_{max} 3376, 2967, 2920, 1711, 1450, 1285, 1228, 1115, 1026, 753, 714 cm^{-1}; ^1H NMR and ^{13}C NMR data, see Tables 3 and 4; HRESIMS *m/z* 434.2326 $[M + H]^+$ (calcd for $C_{27}H_{32}NO_4$: 434.2331).

4.3.9. Anthoroisine I (9)

White powder; [α]20 D +9.4 (*c* 0.75, $CHCl_3$); IR (KBr) ν_{max} 3439, 3166, 2931, 1731, 1654, 1458, 1262, 1242, 1155, 1091, 754 cm^{-1}; ^1H NMR and ^{13}C NMR data, see Tables 3 and 4; HRESIMS *m/z* 442.2590 $[M + H]^+$ (calcd for $C_{26}H_{36}NO_5$: 442.2593).

4.4. X-ray crystallographic analysis

Crystallographic Data for Anthoroisine G (**7**) and Aconicarmicharcutinium A Hydrochloride (**19**), see the Supporting *Information*. Crystal data for **7** and **19** (deposition numbers: CCDC 1559538 and 1,559,539) have been deposited with the Cambridge Crystallographic Data Center. These crystallographic data can be obtained free of charge via www.ccdc.cam.ac.uk/deposit (or from the CCDC, 12 Union Road, Cambridge CB2 1EZ, UK; fax: + 44 1223336033; deposit@ccdc.cam.ac.uk).

4.5. Acid hydrolysis of 4

According to a previously described protocol (Huang et al., 2013), compound **4** (approximately 2 mg) was dissolved in 1 N HCl-dioxane (1:1, 2 mL) and stirred at 90 °C for 3 h. The reaction mixture was diluted with H_2O (3 mL), neutralized with 0.5 N NaOH and then extracted twice with $CHCl_3$. The H_2O layer was concentrated under a stream of nitrogen. Subsequently, 1–(trimethylsilyl) imidazole (0.1 mL) and pyridine (0.2 mL) were added to the residue, and the solution was stirred at 60 °C for 20 min. After the solvent was removed, the residue was partitioned between H_2O and $CHCl_3$. The combined organic phase was dried and analyzed by GC using an L-CP-Chirasil-Val column (0.32 mm × 25 m). D-Glucose was confirmed by comparison of the retention time with that of an authentic standard (7.65 min).

4.6. Cell viability assay

SH–SY5Y (human neuroblastoma cell line) cells were obtained from ATCC, and the cells were maintained in growth medium containing DMEM high–sugar medium (containing 10% calf serum, 100 $KU{\cdot}L^{-1}$ penicillin, and 100 mg L^{-1} streptomycin). The cells were cultured at 37 °C with 5% CO_2 (v/v). MTT and MPP^+ were purchased from Sigma-Aldrich (St. Louis, MO, USA). For experiments, SH–SY5Y cells were seeded in 96-well plates at a density of 1×10^5 cells/mL in 200 μL of medium. After allowing the cells to attach and reach 70–80% confluence, they were treated with different concentrations of the test compounds or MPP^+ for 24 h. The cell viability was estimated by an MTT colorimetric assay. Twenty microliters of MTT (5 mg/mL) was added to each well, and the cells were cultured for 4 h. Subsequently, the medium was removed, and the formazan crystals were dissolved with DMSO. The optical densities (OD) at 490 nm were measured on a microplate reader (TECAN SPECTRA, Wetzlar, Germany) (Wang et al., 2017).

4.7. Acetylcholinesterase inhibition assay

Electric eel acetylcholinesterase (EC 3.1.1.7), acetylthiocholine iodide (ATCI), and 5,5′-dithiobis-2-nitrobenzoic acid (DTNB) were purchased from Sigma-Aldrich (St. Louis, MO, USA). The AChE inhibitory activities were assessed using a 96-well microplate assay modified from Ellman's method (Liu et al., 2013; Ellman et al., 1961). Briefly, 0.2 mM Ellman's reagent (DTNB) (150 μL) in phosphate buffer (0.1 M, pH 8.0), a solution of the test compound (in DMSO, 10 μL) and AChE in H_2O (0.05 U.I./mL, 10 μL) were mixed and incubated for 20 min at 25 °C. Subsequently, ATCI in buffer (10 mM, 10 μL) was added, and the cells were incubated at 37 °C for 20 min. The absorbance was monitored at 405 nm using a microplate reader (TECAN SPECTRA, Wetzlar, Germany). Enzyme inhibitory activity (%) = $[1–(A_{sample}/A_{control})] \times 100$. The IC_{50} values were evaluated using the software package Prism V5.0 (GraphPad Software, San Diego, CA, USA).

Declaration of competing interest

The authors declare no competing financial interest.

Acknowledgments

This research was supported by grants from National Natural Science Foundation of China (81773605), the Interdisciplinary Frontier Basic Research Project of SWJTU (2682017QY04), and the Science and Technology Program of Sichuan, China (2018JY0077).

Appendix A. Supplementary data

Supplementary data to this article can be found online at https://doi.org/10.1016/j.phytochem.2020.112459.

References

Ahmad, H., Ahmad, S., Khan, E., Shahzad, A., Ali, M., Tahir, M.N., Shaheen, F., Ahmad, M., 2017a. Isolation, crystal structure determination and cholinesterase inhibitory potential of isotalatizidine hydrate from *Delphinium denudatum*. Pharm. Biol. 55, 680–686.

Ahmad, H., Ahmad, S., Shah, S.A.A., Latif, A., Ali, M., Khan, F.A., Tahir, M.N., Shaheen, F., Wadood, A., Ahmad, M., 2017b. Antioxidant and anticholinesterase potential of diterpenoid alkaloids from *Aconitum heterophyllum*. Bioorg. Med. Chem. 25, 3368–3376.

Alzheimer's Association, 2018. Alzheimer's disease facts and figures. Alzheimer's Dementia 14, 367–425.

Atta–ur–Rahman, Fatima, N., Akhtar, F., Choudhary, M.I., Khalid, A., 2000. New norditerpenoid alkaloids from *Aconitum falconeri*. J. Nat. Prod. 63, 1393–1395.

Bartus, R.T., Dean, R.L., Beer, B., Lippa, A.S., 1982. The cholinergic hypothesis of geriatric memory dysfunction. Science 217, 408–417.

Bessonova, I.A., Saidkhodzhaeva, S.A., 2000. Hetisane-type diterpenoid alkaloids. Chem. Nat. Compd. 36, 419–477.

Betarbet, R., Sherer, T.B., MacKenzie, G., Garcia–Osuna, M., Panov, A.V., Greenamyre, J. T., 2000. Chronic systemic pesticide exposure reproduces features of Parkinson's disease. Nat. Neurosci. 3, 1301–1306.

Cai, L., Song, L., Chen, Q.H., Liu, X.Y., Wang, F.P., 2010. Piepunine, A novel bis-diterpenoid alkaloid from the roots of *Aconitum piepunense*. Helv. Chim. Acta 93, 2251–2255.

Cheng, Z.B., Li, Y.L., Xu, W., Liu, W., Liu, L.J., Zhu, D.G., Kang, Y., Luo, Z.H., Li, Q., 2019. Three new cyclopiane-type diterpenes from a deep-sea derived fungus *penicillium* sp. ypga11 and their effects against human esophageal carcinoma cells. Bioorg. Chem. 91, 103129.

Ding, L.S., Wu, F.E., Chen, Y.Z., 1992. Diterpenoid alkaloids from *Aconitum gymnandrum*. Acta Pharm. Sin. 27, 394–396.

Duan, X.Y., Zhao, D.K., Shen, Y., 2019. Two new bis-C_{20}-diterpenoid alkaloids with anti-inflammation activity from *Aconitum bulleyanum*. J. Asian Nat. Prod. Res. 21, 323–330.

Ellman, G.L., Courtney, K.D., Andres, V., Featherstone, R.M., 1961. A new and rapid colorimetric determination of acetylcholinesterase activity. Biochem. Pharmacol. 7, 88–95.

Fan, X.R., Yang, L.H., Liu, Z.H., Lin, L.M., Li, C., Guo, S.S., Wang, Z.M., Wang, Z.J., Sui, F., 2019. Diterpenoid alkaloids from the whole plant of *Aconitum tanguticum* (Maxim.) Stapf. Phytochemistry 160, 71–77.

Giacobine, E., Becker, R., 1997. Alzheimer's Disease: Molecular Biology to Therapy. Birkhäuser Boston, Boston, p. 187.

Giacobini, E., 2000. Cholinesterase inhibitors stabilize alzheimer disease. Neurochem. Res. 25, 1185–1190.

Gonzalez, A.G., De la Fuente, G., Reina, M., Diaz, R., Timón, L., 1986. ^{13}C NMR spectroscopy of some hetisine subtype C_{20}-diterpenoid alkaloids and their derivatives. Phytochemistry 25, 1971–1973.

He, J.B., Luan, J., Lv, X.M., Rui, D.Y., Tao, J., Wang, B., Niu, Y.F., Ju, H.P., 2017. Navicularines A-C: new diterpenoid alkaloids from *Aconitum naviculare* and their cytotoxic activities. Fitoterapia 120, 142–145.

He, L., Chen, Y.Z., Ding, L.S., Li, B.G., 1997. Alkaloids from *tongolo larkspur* (*Delphinium tongolese*). Chin. Tradit. Herb. Drugs 28, 392–395.

Huang, S., Zhou, X.L., Wang, C.J., Wang, Y.S., Xiao, F., Shan, L.H., Guo, Z.Y., Weng, J., 2013. Pyrrolizidine alkaloids from *Liparis nervosa* with inhibitory activities against LPS-induced NO production in RAW 264.7 macrophages. Phytochemistry 93, 154–161.

Ibrahim, M.A., Na, M., Oh, J., Schinazi, R.F., McBrayer, T.R., Whitaker, T., Doerksen, R. J., Newman, D.J., Zachos, L.G., Hamann, M.T., 2013. Significance of endangered and threatened plant natural products in the control of human disease. Proc. Natl. Acad. Sci. U. S. A. 110, 16832–16837.

Jiang, B.Y., Lin, S., Zhu, C.G., Wang, S.J., Wang, Y.N., Chen, M.H., Zhang, J.J., Hu, J.F., Chen, N.H., Yang, Y.C., Shi, J.G., 2012. Diterpenoid alkaloids from the lateral root of *Aconitum carmichaelii*. J. Nat. Prod. 75, 1145–1159.

Jiang, Q., Pelletier, S.W., 1991. Two new diterpenoid alkaloids from *Aconitum palmatum*. J. Nat. Prod. 54, 525–531.

Lin, L., Chen, D.L., Liu, X.Y., Chen, Q.H., Wang, F.P., Yang, C.Y., 2009. Bis-diterpenoid alkaloids from *Aconitum tanguticum* var. *trichocarpum*. Nat. prod. Commun. 4, 897–901.

Liu, J.Q., Peng, X.R., Li, X.Y., Li, T.Z., Zhang, W.M., Shi, L., Han, J., Qiu, M.H., 2013. Norfriedelins A–C with acetylcholinesterase inhibitory activity from *Acerola Tree* (*Malpighia emarginata*). Org. Lett. 15, 1580–1583.

Malak, L.G., Ibrahim, M.A., Moharram, A.M., Pandey, P., Tekwani, B., Doerksen, R.J., Ferreira, D., Ross, S.A., 2018. Antileishmanial carbasugars from geosmithia langdonii. J. Nat. Prod. 81, 2222–2227.

McKay, D.B., Chang, C., González–Cestari, T.F., McKay, S.B., Ei–Hajj, R.A., Bryant, D.L., Zhu, M.X., Swaan, P.W., Arason, K.M., Pulipaka, A.B., Orac, C.M., Bergmeier, S.C., 2007. Analogs of methyllycaconitine as novel noncompetitive inhibitors of nicotinic receptors: pharmacological characterization, computational modeling, and pharmacophore development. Mol. Pharmacol. 71, 1288–1297.

Meng, X.H., Guo, Q.L., Zhu, C.G., Shi, J.G., 2017a. Unprecedented C_{19}-diterpenoid alkaloid glycosides from an aqueous extract of "fu zi": neoline 14-O-L-arabinosides with four isomeric L-anabinosyls. Chin. Chem. Lett. 28, 1705–1710.

Meng, X.H., Jiang, Z.B., Guo, Q.L., Shi, J.G., 2017b. A minor arcutine-type C_{20}-diterpenoid alkaloid iminium constituent of "fu zi". Chin. Chem. Lett. 28, 588–592.

Pelletier, S.W., Iyer, K.N., Bhalla, V.K., Newton, M.G., Aneja, R., 1970. Crystal structure of the diterpene alkaloid hetidine. J. Chem. Soc. D 7, 393.

Pelletier, S.W., Mody, N.V., 1979. An unusual rearrangement of ajaconine: an example of a "disfavored" 5-endo-trigonal ring closure. J. Am. Chem. Soc. 101, 492–494.

Przedborski, S., Jackson–Lewis, V., 1998. Mechanisms of MPTP toxicity. Mov. Disord. 13, 35–38.

Shihabuddin, L.S., Brundin, P., Greenamyre, J.T., Stephenson, D., Sardi, S.P., 2018. New frontiers in Parkinson's disease: from genetics to the clinic. J. Neurosci. 38, 9375–9382.

Singer, T.P., Ramsay, R.R., 1990. Mechanism of the neurotoxicity of MPTP an update. FEBS Lett. 274, 1–8.

Tang, Q.F., Liu, J.H., Xue, J., Ye, W.C., Zhang, Z.J., Yang, C.H., 2008. Preparative isolation and purification of two new isomeric diterpenoid alkaloids from *Aconitum coreanum* by high-speed counter-current chromatography. J. Chromatogr. B 872, 181–185.

Tarasoff-Conway, J.M., Carare, R.O., Osorio, R.S., Glodzik, L., Butler, T., Fieremans, E., Axel, L., Rusinek, H., Nicholson, C., Zlokovic, B.V., Frangione, B., Blennow, K., Ménard, J., Zetterberg, H., Wisniewski, T., de Leon, M.J., 2015. Clearance systems in the brain-implications for Alzheimer disease. Nat. Rev. Neurol. 11, 457–470.

Tashkhodzhaev, B., Yusupova, M., Salimov, B.T., Ibragimov, B.T., 1992. Crystal and molecular structure of the hydrochloride of the diterpene alkaloid hetisine. J. Inclusion Phenom. Mol. Recognit. Chem. 14, 311–316.

Wang, F.P., Chen, Q.H., Liu, X.Y., 2010. Diterpenoid alkaloids. Nat. Prod. Rep. 27, 529–570.

Wang, F.P., Liang, X.T., 2002. The Alkaloids: Chemistry and Biology, vol. 59. Elsevier Science, New York, p. 5.

Wang, F.P., Peng, C.S., Yu, K.B., 2000. Racemulosine, a novel skeletal C_{20}-diterpenoid alkaloid from *Aconitum racemulosum* Franch var. *pengzhouense*. Tetrahedron 56, 7443–7446.

Wang, F.P., Yan, L.P., 2007. Campylopin from *Delphinium campylocentrum*, the first hetidane C_{20}-diterpene, suggests a new alkaloid biogenetic pathway. Tetrahedron 63, 1417–1420.

Wang, G., Zhu, L.J., Zhao, Y.Q., Gao, S.Y., Sun, D.J., Yuan, J.Q., Yao, X.S., 2017. A natural product from Cannabis sativa subsp sativa inhibits homeodomain-interacting protein kinase 2 (HIPK2), attenuating MPP^+-induced apoptosis in human neuroblastoma SH-SY5Y cells. Bioorg. Chem. 72, 64–73.

Wang, W.T., 1979. Flora Reipublicae Popularis Sinicae, vol. 27. Science Press, Beijing, p. pp323.

Wangchuk, P., Bremner, J.B., Samosorn, S., 2007. Hetisine-type diterpenoid alkaloids from the bhutanese medicinal plant *Aconitum orochryseum*. J. Nat. Prod. 70, 1808–1811.

Yusupova, I.M., Salimov, B.T., Tashkhodzhaev, B., 1992. Tadzhaconine - a new C_{20} diterpene alkaloid from *Aconitum zeravschanicum*. Chem. Nat. Compd. 28, 335–339.

Zhang, J.F., Li, Y., Gao, F., Shan, L.H., Zhou, X.L., 2019. Four new C_{20}-diterpenoid alkaloids from *Aconitum rotundifolium*. J. Asian Nat. Prod. Res. 21, 716–724.

Zhang, J.F., Dai, R.Y., Shan, L.H., Chen, L., Xu, L., Wu, M.Y., Wang, C.J., Huang, S., Zhou, X.L., 2016. Iliensines A and B: two new C_{19}-diterpenoid alkaloids from *Delphinium iliense*. Phytochem. Lett. 17, 299–303.

Zhang, S.S., Ma, Q.Y., Huang, S.Z., Dai, H.F., Guo, Z.K., Yu, Z.F., Zhao, Y.X., 2015. Lanostanoids with acetylcholinesterase inhibitory activity from the mushroom *Haddowia longipes*. Phytochemistry 110, 133–139.

Zhang, Z.T., Chen, D.L., Chen, Q.H., Wang, F.P., 2013. Bis-diterpenoid alkaloids from *Aconitum tanguticum* var. *trichocarpum*. Helv. Chim. Acta 96, 710–718.

Zhou, X.L., Chen, D.L., Chen, Q.H., Wang, F.P., 2005. C_{20}-diterpenoid alkaloids from *Delphinium trifoliolatum*. J. Nat. Prod. 68, 1076–1079.